Zhu *et al.*
Biotechnology for Biofuels and Bioproducts (2025) 18:51
https://doi.org/10.1186/s13068-025-02645-2

Biotechnology for Biofuels and Bioproducts

RESEARCH

Open Access

Alternative Splicing of *BnABF4L* Mediates Response to Abiotic Stresses in Rapeseed (*Brassica napus* L.)

Ruijia Zhu[1†], Chu Yue[1†], Shifan Wu[1], Mingting Wu[1], Ziyue Xu[1], Xiaoqun Liu[1], Rui Wang[1] and Maolin Wang[1*]

Abstract

ABRE BINDING FACTOR 4 (*ABF4*) is a pivotal regulatory gene in the abscisic acid (ABA) signaling pathway, and changes in its expression levels can modulate the plant's stress resistance. To further explore the specific regulatory mechanisms of alternative splicing (AS) in the ABA signaling pathway and to identify new breakthroughs for breeding high stress-resistant varieties of *Brassica napus*, we identified 17 homologous genes of *ABF4* in the genome. Utilizing bioinformatics techniques, we analyzed their motifs, conserved domains, and *cis*-acting elements of their promoters. Through transcriptome data from the stress-tolerant dwarf strain *ndf2* and its parental line *3529*, we uncovered a significantly differentially expressed *ABF4* gene, which we named *BnABF4L*. Subsequently, we analyzed the AS events of *BnABF4L* under normal growth conditions and different abiotic stresses, as well as the impact of different transcript variants' 5′ untranslated region (5′UTR) on gene translation. *BnABF4L* undergoes alternative 3′ splice site (A3SS) selection to produce three transcripts (V1-V3) with divergent 5′UTRs. While V1 translation is suppressed by upstream ORFs (uORFs), V2/V3 exhibit enhanced translational efficiency. Under stress, *ndf2* shifts splicing toward V3, circumventing uORF-mediated repression to upregulate stress-adapted isoforms. We validated the inhibitory effect of upstream open reading frames (uORFs) on protein-coding open reading frame (pORFs) and, based on the collective experimental results, proposed the flexible regulatory mechanism of AS events of *BnABF4L* in response to stress. Our findings provide new insights for future studies on stress resistance in rapeseed as well as for research on the regulation of alternative splicing mechanisms in the ABA signaling pathway.

Keywords ABA signaling pathway, Alternative splicing, Abiotic stress, UORF

Background

Brassica napus (2n = 38, AACC) is one of the largest oilseed crops in the world, holding significant economic and agricultural value[1]. It not only provides a source of edible oil and protein but also plays a crucial role in biofuel and chemical raw materials. However, in recent years, due to factors such as climate change and human activities, *B. napus* has been increasingly subjected to severe abiotic stresses, such as drought, extreme temperatures, salinization, and heavy metal contamination[2]. Through prolonged natural selection, *B. napus* have gradually evolved complex mechanisms for survival and adaptation in response to the intricate and dynamic environmental conditions. The defense mechanisms of plants against stress primarily rely on the regulation of resistance gene expression[3]. This regulation process can be further subdivided into three levels: transcription, translation, and protein processing.

†Ruijia Zhu and Chu Yue contributed equally to this work.

*Correspondence:
Maolin Wang
mlwang@scu.edu.cn
[1] Key Laboratory of Bio-Resource and Eco-Environment of Ministry of Education, College of Life Sciences, Sichuan University, Chengdu 610065, Sichuan, China

In plants, alternative splicing (AS) serves as a crucial mechanism for gene regulation and adaptation to environmental changes[4]. It generates multiple transcripts through various splicing modes, thereby enriching the functional diversity of the plant genome[5]. According to its regulatory mechanisms, alternative splicing can be classified into seven major categories: exon skipping (ES)[6], intron retention (IR)[7], mutually exclusive exon (MEE)[8], alternative 5'splice site (A5SS)[9], alternative 3'splice site (A3SS)[10], alternative first exon (AFE)[11] and alternative last exon (ALE)[12].

Many studies have demonstrated the significant role of alternative splicing in regulating plant resistance to abiotic stresses[13]. The production of alternative splicing isoforms is closely associated with plant responses to abiotic stresses[14]. For instance, the splicing regulator *PCP* (PORCU-PINE) in *Arabidopsis thaliana* functions as a temperature-sensitive modulator during plant development, influencing the expression of *AtCLV3* (CLAVATA3) and *AtWUS* (WUSCHEL)[15]. In rice, *OsHSFA2 d* encodes a heat shock transcription factor, which undergoes alternative splicing to produce two protein isoforms, *OsHSFA2 dI* and *OsHSFA2 dII*[16]. Under conditions of heat stress, *OsHSFA2 d* tends to prioritize the generation of the transcriptionally active form *OsHSFA2 dI*. This variant then governs the expression of downstream stress-responsive genes, thereby assisting the plant in adapting to extreme temperatures. Differential physiological states lead to changes in alternative splicing patterns, influencing the types and abundance of gene expression products and prompting appropriate responses to external stimuli, ultimately ensuring the organism's survival. The alternative splicing theory provides a robust explanation for the paradox between small genomes and large transcriptomes, enriching the variety of gene expression products and enabling the formation of complex and intricate metabolic regulatory networks within organisms[17].

Abscisic acid (ABA) plays a vital role in modulating plant growth by engaging in numerous metabolic pathways[18]. ABA responsive element-binding factors (*ABFs/AREB*) are important transcription factors within the *bZIP* family[19], characterized by a typical leucine zipper domain[20]. They can interact with *ABRE* motifs present in downstream gene promoters, thereby modulating the expression patterns of multiple genes and directly influencing various plant traits[21]. In *Arabidopsis*, *ABFs* consist of subtypes *ABF1*, *ABF2*, *ABF3*, and *ABF4*[22]. These different *ABF* subtypes exhibit both overlapping and distinct functions. *ABF1* is involved in the response to water stress[23] and cold stress[24] in *Arabidopsis*. *ABF2*, *ABF3*, and *ABF4* serve as primary regulators of the ABA signaling pathway during drought[25] and osmotic stress conditions[26], displaying diverse functionalities. In *Arabidopsis*, overexpression of *ABF4* activates *PDC1*, thereby promoting ROS accumulation in seeds, resulting in increased sensitivity of *Arabidopsis* to ABA. Consequently, seed germination in *Arabidopsis* is inhibited, plant growth rate is slowed, but resistance to adverse conditions is enhanced[27]. Plants rely on both stress-responsive genes and alternative splicing to manage responses to abiotic stresses. Ongoing research in this area enhances our grasp of the molecular mechanisms involved in plant adaptation to challenging environments, thereby offering theoretical and technical backing for developing stress-resistant crop varieties.

In this study, we identified the members of the *ABF4* gene family from the genome of *B. napus* and selected a potentially important gene, *BnABF4L*, which undergoes alternative splicing and plays a crucial role in the stress response of *B. napus*. We investigated the expression pattern of this gene and its response to abiotic stress, aiming to gain insights into the specific regulatory mechanisms of metabolic pathways in *B. napus* and provide valuable references for breeding new rapeseed strains with desirable traits.

Results

Identification and bioinformatics analysis of *ABF4 s* genes in *B. napus*

The phylogenetic tree of multi-species *ABF4* genes reveals that all identified genes can be divided into four clades. Among them, five genes are closely related to *AtABF4*, two genes cluster with *AtABF3*, ten genes are distantly related to *AtABFs*, and two genes show closer relationships to the *ABF4* gene in maize (Fig. 1b).

ndf2 is a stress-resistant variety derived from the *3529* mutation, as shown in previous studies (Fig. 1a). We analyzed the expression levels of 17 *ABF4* genes in different periods and tissues of two strains using the donated transcriptome data. The heatmap results indicated that most genes exhibit similar expression patterns in both *ndf2* and *3529*. However, *BnC03 ABF4.13* is an exception, with significantly different expression levels between the two strains (Fig. 1c). It showed higher expression level in *ndf2* compared to *3529* in any stage and tissue.

A correlation analysis between qRT-PCR data and RNA-seq FPKM values showed that the expression of the four selected genes was highly correlated (Fig. 1d). The range of R-value was between 0.72–0.92.

Motifs, conserved domains, and *cis*-acting elements were analyzed based on their phylogenetic relationships. Most of the ORFs were 800–1300 bp in length. We selected the top ten motifs that appeared in BnABF4 s proteins, and the specific motif sequences are provided

in the attached figure (Fig. 1e). The results indicated that all proteins contain motif 1-motif 4, motif 8, and motif 9. BnC06 ABF4.3 does not contain motif 5, while BnA04 ABF4.9 and BnC04 ABF4.10 do not contain motif 6, motif 7. Interestingly, apart from BnC03 ABF4.13, the other four proteins that are closely related to AtABF4 contain all ten motifs.

From the perspective of conserved domains, all proteins contain bZIP_plant_BZIP46, a DNA-binding and dimerization domain, which is a type of basic leucine zipper (bZIP) domain involved in developmental and physiological processes under light, hormone, and temperature stress. Interestingly, only BnC04 ABF4.6 contains a COG5222 superfamily, an uncharacterized conserved protein that includes a RING zinc finger (Fig. 1e).

Furthermore, we categorized all *cis*-acting elements into four types: abiotic and biotic stress-responsive elements, phytohormone-responsive elements, light-responsive elements, and growth and development-responsive elements. Various *cis*-acting elements have been identified, including *ARE* (Antioxidant Responsive Element), *MYB/MYC* motif (DNA-binding domain), *STRE* (stress response element), *ERE* (estrogen-responsive element), etc. These elements participates in the regulation of gene expression related to growth, development, reproduction, and environmental responses. *P-box* (gibberellin-responsive element) and *ABRE* (ABA responsive element) are widely present in the *ABF4* genes. Additionally, light-responsive elements such as AT1-motif, Box 4, G-box, and GT1-motif are also abundantly present in the *ABF4* (Fig. 1g). These results indicated that *BnABF4* gene members are involved in hormone signaling pathways, stress response, and light response processes, playing an important role in abiotic stress responses in *B. napus*.

Gene structure and alternative splicing analysis of *BnABF4L*

Analysis of the gene expression patterns of selected 17 *BnABF4* in *ndf2* and *3529* revealed significant differences in expression levels of *BnC03 ABF4.13*, which is closely related to *AtABF4*, in both strains (Fig. 1c). Notably, this gene exhibited higher expression levels at various stage in *ndf2* (Fig. 1f). Furthermore, combined with bioinformatics predictions, these findings suggested that this gene may be more involved in abiotic stress compared to other *BnABF4*. Consequently, we selected this gene for further functional analysis and validation of our hypothesis, and designated it as *BnABF4L*.

Subsequently, we successfully cloned the DNA sequence of the gene as well as the three transcript sequences generated through alternative splicing, and labeled them as *BnABF4L*-V1, *BnABF4L*-V2, and *BnABF4L*-V3, the subsequent text will be abbreviated as V1, V2, and V3. (Fig. 2a). Through gene structure analysis, it was found that the full length of the *BnABF4L* is 2528 bp, consisting of five exons and four introns arranged alternately (Supplementary Figure S1). The introns are all the GU-AG type, with the boundaries of intron 2, 3, and 4 being fixed. During pre-mRNA processing to form three mature transcripts through alternative splicing, intron 2, 3, and 4 are all excised. However, intron 1 has a fixed 5'splice site, but three alternative 3'splice sites (A3SS). During splicing, the spliceosome recognizes different A3SS and excises them, leading to changes in the lengths of intron1 and exon 2. A longer intron 1 results in a shorter exon 2 (Fig. 1e).

V1 has a total length of 1950 bp, with a 588 bp 5'UTR, a 1065 bp CDS, and a 298 bp 3'UTR. It encodes a protein consisting of 354 amino acids. This transcript is formed by the splicing of four exons. During the splicing process of this transcript, the spliceosome selects A3SS-1 as the 3'end boundary of intron 1, resulting in the excision of exon1 and intron 1 together. This AS event belongs to variable splicing of exon 1. It is worth noting that the 5'UTR sequence of V1 contains seven start codons (ATG).

V2 has a length of 1542 bp, with a 180 bp 5'UTR, a 1065 bp CDS, and a 298 bp 3'UTR. It encodes a protein consisting of 354 amino acids. This transcript includes

(See figure on next page.)

Fig. 1 Identification, bioinformatics and relative expression level of *ABF4* in *B. napus*. **a** Heat stress treatment in *ndf2* and *3529* strains. Scale bars = 10 cm. **b** Phylogenetic analysis of *ABF4* in *Arabidopsis thaliana*, *Brassica napus*, *Nicotiana benthamiana*, *Solanum lycopersicum*, *Vitis vinifera*, and *Zea mays*. It was constructed by maximum likelihood (ML) method based on multiple sequence alignment of 25 amino acid sequences of *ABF4*. **c** Expression of 17 *BnABF4* in different tissues and in *3529* and *ndf2* strains. Heatmaps were displayed with $\log_2$ values for each gene. The color scale represents the relative expression levels from low (blue) to high (red). **d** Correlation analysis between RNA-seq data and qRT-PCR data. Student's *t*-test was used to calculate significance. **e** Distribution of motif elements and conserved domains, the colored bars and boxes represent the location of different motifs and domains respectively. **f** The relative expression profile of *BnABF4L* in three tissues within the *3529* and *ndf2* strains. Different letters above the bars indicate significantly different values ($p < 0.05$) calculated using one-way analysis of variance (ANOVA) followed by Tukey's multiple range. **g** Cis-elements analysis of the *BnABF4* genes family promoter regions 1500 bp upstream of the initial codons. The number of cis-acting elements corresponding to the horizontal axis that are present in the promoter region. The color scale represents the numbers from low (white) to high (blue)

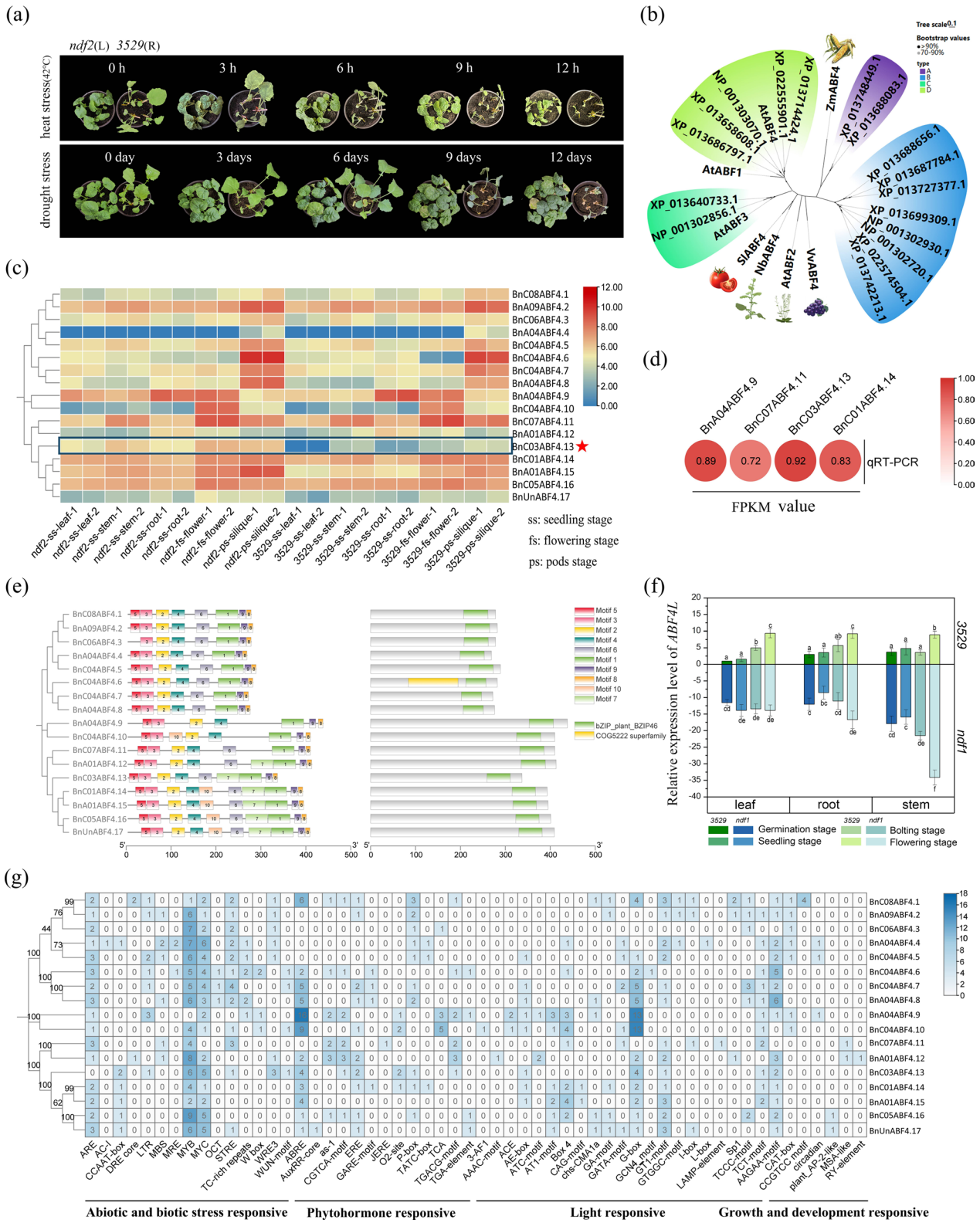

Fig. 1 (See legend on previous page.)

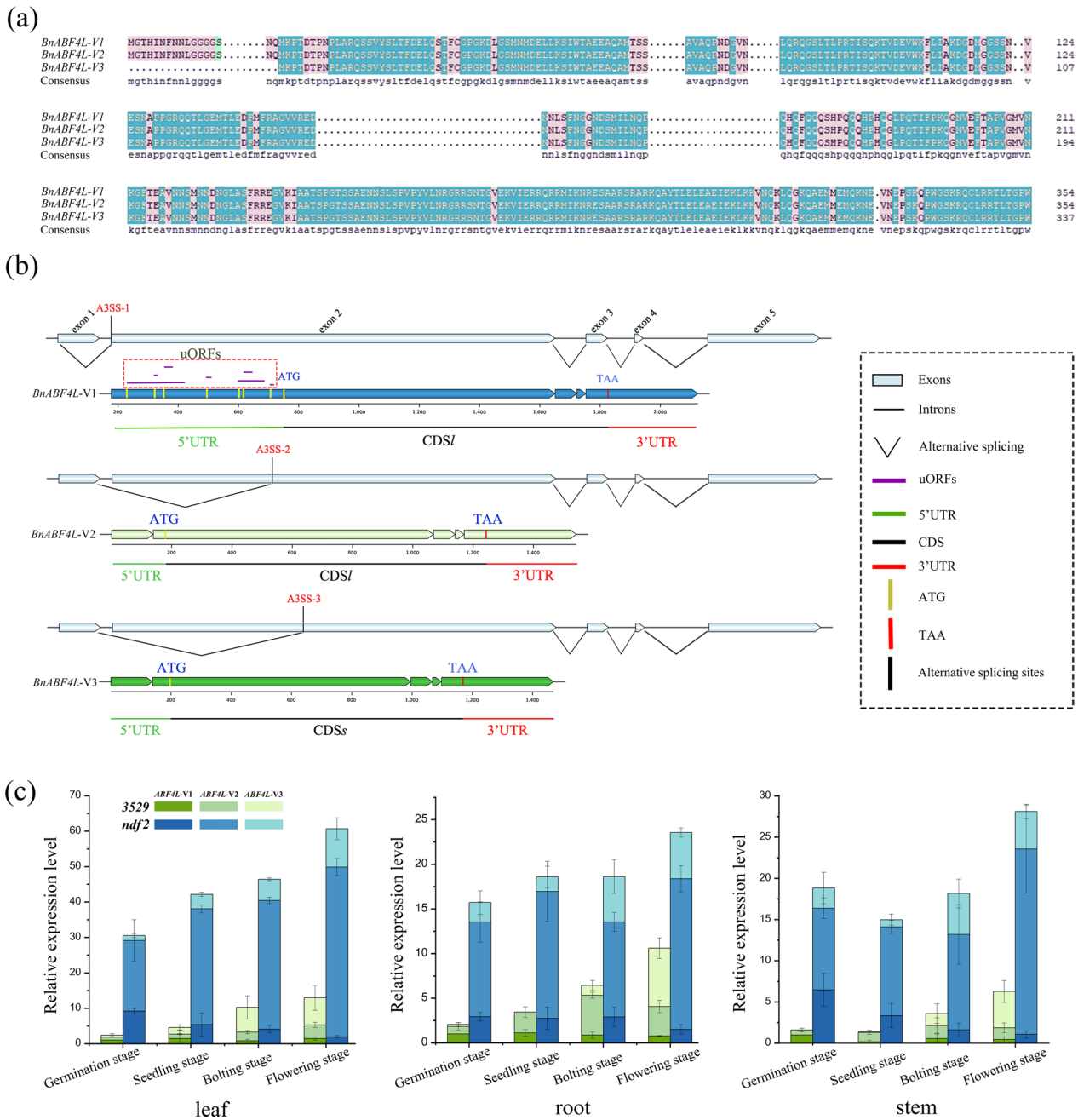

Fig. 2 Alternative splicing events analysis and relative expression level of *BnABF4L*-V1/V2/V3. **a** Amino acid sequences alignment of three transcripts of *BnABF4L* and *AtABF4*. **b** Exon splicing pattern of three transcripts of *BnABF4L*. **c** The grouped stacked error bar chart displays the relative expression levels of three transcripts in different tissues and developmental periods within the *3529* and *ndf2* strain

all five exons of the *BnABF4L*. Due to multiple A3SS at the 3'end of intron 1, the spliceosome selects A3SS-2 as the 3'splice site during splicing, leading to the excision of intron 1 and a portion of the sequence originally belonging to exon 2. As a result, exon 2 becomes shorter. This type of alternative splicing belongs to 3'end variable splicing. The CDS region and 3'UTR of V1 and V2 are identical. The only difference lies in the 5'UTR of V2, which lacks redundant ATG, resulting in the translation initiation site being the first ATG within the sequence.

V3 has a length of 1469 bp, with a 158 bp 5'UTR, a 1014 bp CDS, and a 298 bp 3'UTR. It encodes a protein consisting of 337 amino acids. This transcript includes all five exons of the *BnABF4L*. During the splicing process

of this transcript, the spliceosome selects"A3SS-3"as the 3'end boundary of intron 1, resulting in the excision of intron 1 and a portion of the sequence originally belonging to exon 2. As a result, exon 2 becomes shorter. This alternative splicing event belongs to 3'end variable splicing. V3 is only identical to the previous transcripts in terms of its 3'UTR. There are differences in both the 5'UTR and CDS regions compared to the previous transcripts. The 5'UTR of this transcript also does not contain any redundant ATG (Fig. 2b).

Based on the above, although the gene undergoes alternative splicing to generate three mature transcripts, there are only two CDS. The CDS of V1 and V2 is longer at 1065 bp, and named as CDS*l* (*BnABF4L*-CDS-*long*). The CDS of V3 is shorter at 1014 bp, and named as CDS*s* (*BnABF4L*-CDS-*short*). The difference between CDS*l* and CDS*s* lies in their 5'end, where CDS*l* has an additional 51 bp compared to CDS*s*.

The expression patterns of *BnABF4L* and its three transcript variants

To obtain further insights into the expression pattern of *BnABF4L* in *B. napus*, we measured the relative expression levels of *BnABF4L* in roots, stems, and leaves of two strains, *ndf2* and *3529*, at four developmental stages: germination, seedling, bolting, and flowering. (Fig. 2c). The results indicated that in any given stage and tissue, the relative expression level of *BnABF4L* was significantly higher in *ndf2* than in *3529*. In *3529*, the relative expression level of *BnABF4L* in all three tissues steadily increased over time, while in *ndf2*, it maintained a relatively high expression level with no significant changes.

The relative contribution of each of the three splice variants to the total amount of *BnABF4L* expression was evaluated with qPCR assays that were specific for each transcript. The results showed that in *ndf2*, the expression level of V1 exhibited a decreasing trend, while the expression level of V2 remained relatively stable. On the other hand, the expression level of V3 gradually increased. In *3529*, the expression level of V1 remained consistently low, while the expression levels of V2 and V3 showed an increasing trend, especially V3. This pattern is not identical to what was observed in *ndf2*.

Under normal growth conditions, the more stress-tolerant variety *ndf2* showed significantly higher gene expression levels of *BnABF4L*, with V2 being the dominant isoform. To further investigate the role of *BnABF4L* in response to abiotic stress, we subjected *ndf2* to cold, heat, osmotic, and drought stress, and designed specific qRT-PCR primers for the three splice variants of *ABF4L* to measure their relative expression levels. The results showed that under all four abiotic stress conditions, the expression levels of V2 and V3 were increased to some extent, while the expression level of V1 continued to decrease (Fig. 3). However, in the case of high temperature and high osmotic stress, the expression levels of V2 and V3 did not consistently remain elevated after reaching a peak, but instead showed a subsequent decrease. We speculate that the reason for this phenomenon may be that prolonged exposure to high temperature or high osmotic environments causes severe damage to the plants, and the plant's responses are unable to restore the damage caused by the stressful conditions. As a result, it severely affects the plant's vitality, leading to an overall decline in physiological and biochemical metabolic levels within the plants.

Transcriptional activation function of *BnABF4L* protein

To determine if *BnABF4L* is transcriptionally functional, subcellular localization, as well as transcriptional activation validation experiments were conducted on the two transcript variants (Fig. 4d). Results showed that both CDS*l* and CDS*s* localized in the nucleus (Fig. 4c). Both proteins, similar to *AtABF4*, possess a typical leucine zipper structure, which typically participates in DNA binding and transcriptional regulation, among other biochemical processes.

These results indicate that *BnABF4L* possesses transcriptional activation function, consistent with general characteristics of bZIP-type transcription factors.

Impact of 5'UTRs on translation efficiency of *BnABF4L* transcripts

UTRs are special sequences present on mature mRNA molecules, outside the protein-coding region. 5'UTR can potentially affect the recruitment of ribosomes to mRNA and even interfere with the selection of translation initiation sites by ribosomes[28]. On the other hand, 3'UTR primarily impact the stability of mRNA molecules[29].

Based on previous analysis, it was found that the mature mRNAs of V1, V2, and V3 have distinct 5'UTRs but share the same 3'UTR. To investigate the impact of different 5'UTRs of *BnABF4L* transcripts on translation efficiency, we fused their 5'UTRs individually with *eGFP* or *GUS* reporter genes, then incorporated them into the pBI-121 vector and transiently transformed into tobacco leaves. Translation efficiency was then assessed qualitatively and quantitatively by measuring eGFP fluorescence intensity and determining GUS enzyme activity.

The results showed minimal fluorescence was observed in tobacco leaves transformed with V1-5'UTR-eGFP, while stronger observable fluorescence signals were detected in leaves transformed with V2-5'UTR-eGFP compared to V3-5'UTR-eGFP (Fig. 4b). V2-5'UTR-GUS

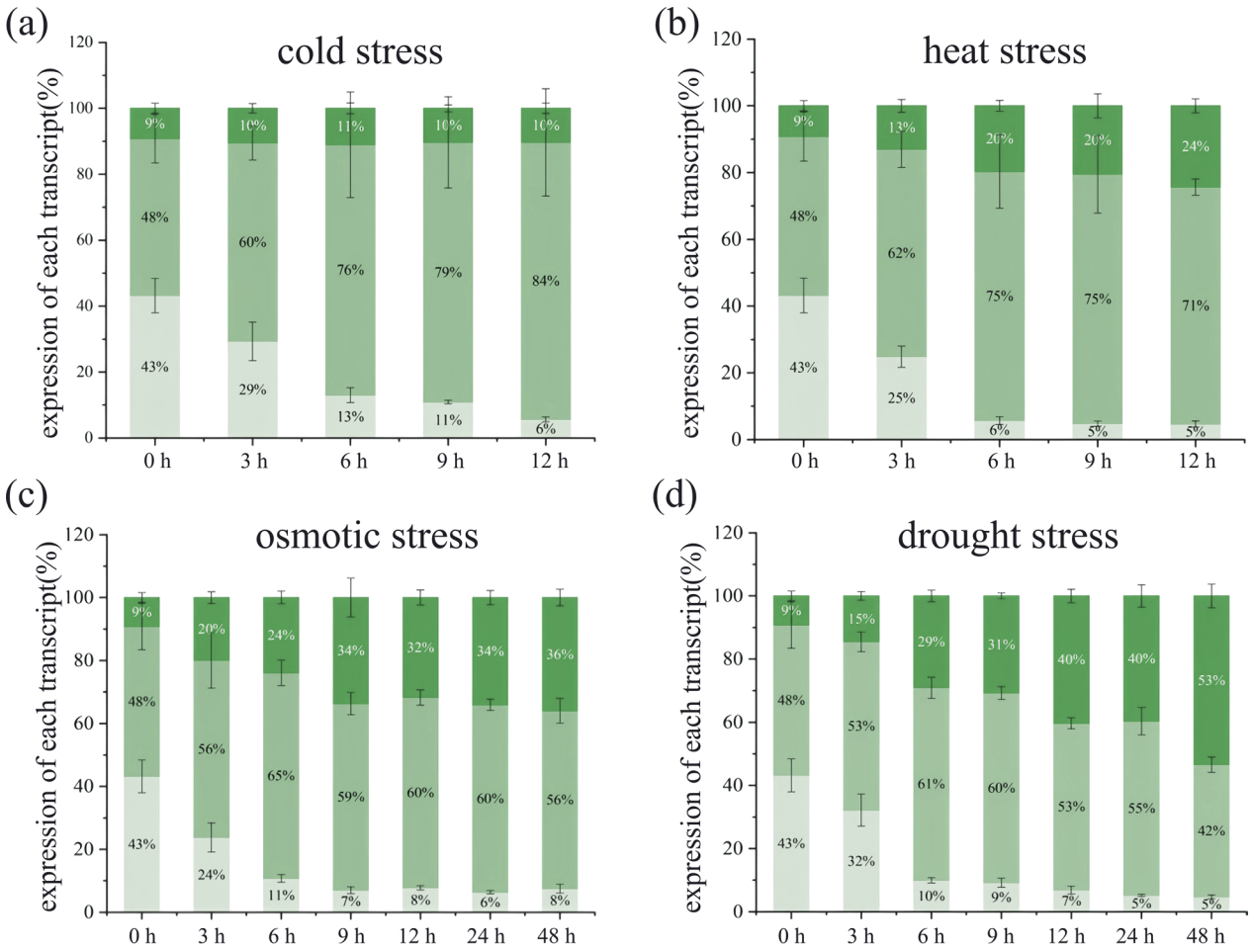

Fig. 3 Analysis of AS events of *BnABF4L* under different abiotic stress. Percentage stacked bars showing frequence of three transcripts of *BnABF4L* under different treatments in *ndf2* strain. **a** Cold stress treatment. **b** Heat stress treatment. **c** Osmtic stress treatment. **d** Drought stress treatment

exhibited the strongest staining, followed by V3-5'UTR-GUS, with *35S* promoter-driven GUS gene staining falling between the two. Minimal staining was observed for V1-5'UTR-GUS (Fig. 4a). GUS enzyme activity assays yielded results consistent with the staining, with V1-5'UTR-GUS transgenic plants exhibiting extremely low GUS protein enzyme activity. In contrast, V2-5'UTR-GUS transgenic plants displayed the highest GUS protein enzyme activity, approximately 62.12 times higher than that of V1-5'UTR-GUS transgenic plants, and approximately 1.88 times higher than that of V3-5'UTR-GUS transgenic plants (Fig. 4a). These findings suggested that the 5'UTR of V1 exerted a significant inhibitory effect on translation, hindering the translation of CDS*l* in V1. On the other hand, the 5'UTRs of V2 and V3 do not exhibit a substantial inhibitory effect on translation and, importantly, the 5'UTR of V2 significantly promotes protein expression.

Response of the three *BnABF4L* transcripts to ABA and abiotic stress.

To further investigate the response of the three *BnABF4L* transcripts to ABA and abiotic stress, each of them were constructed onto overexpression vectors and transformed into *Arabidopsis* using the floral dip transformation method. Finally, we selected three lines with the highest relative expression levels from each transgenic plant as the experimental subjects (Fig. 5d). The results showed that after four weeks of growth, there were no significant differences in phenotype among *Col-0 Arabidopsis*, OE::*BnABF4L*-V1 and OE::*BnABF4L*-V3 overexpressing *Arabidopsis* plants. While as the overexpressing plants of V2 exhibited a dwarf and shortened petiole and root growth status (Fig. 5a, b), with a rosette leaf diameter approximately 30% larger than the other three types of *Arabidopsis* (Fig. 5c).

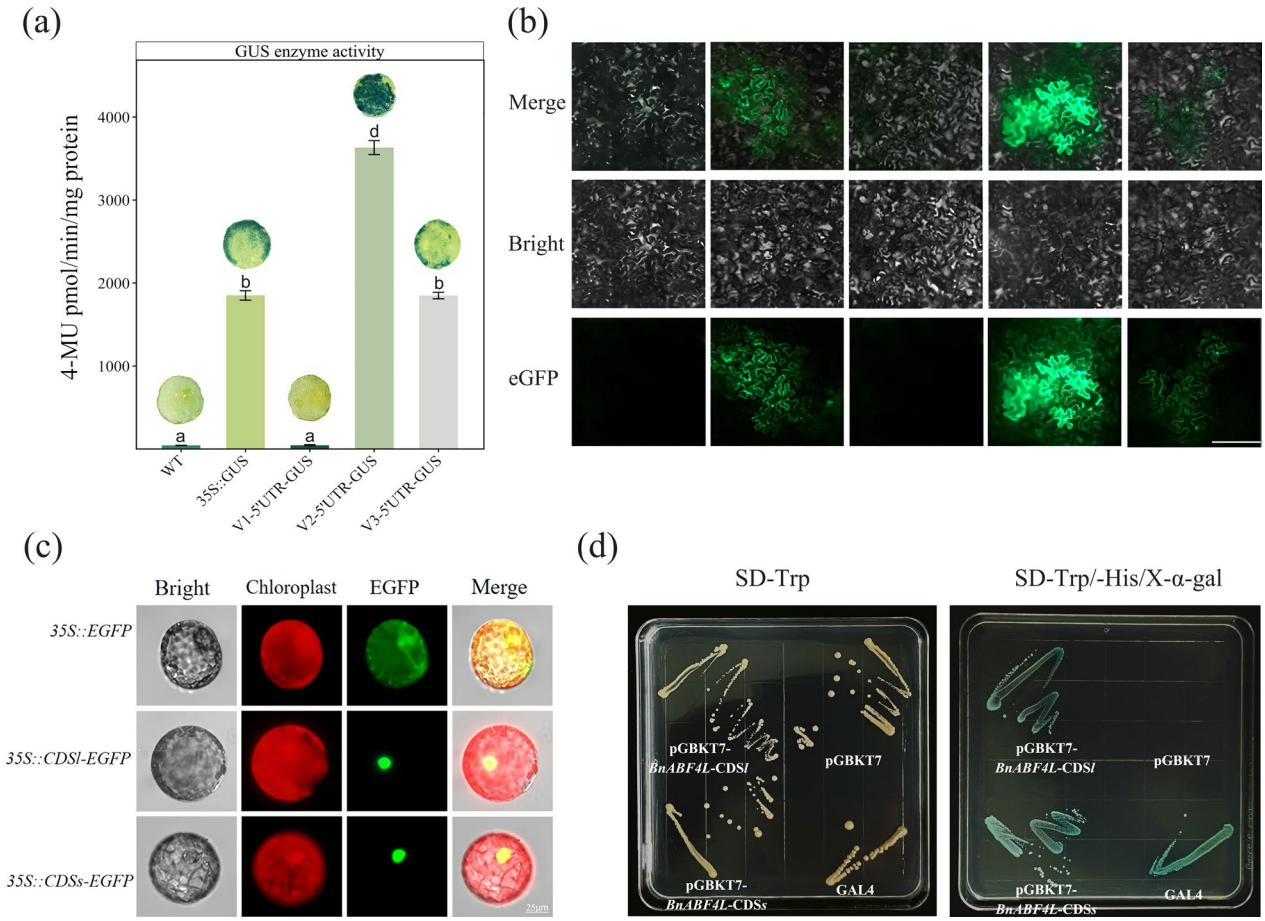

Fig. 4 Effects of three 5′UTRs on reporter gene translation respectively and transactivation. **a** Measurement of GUS enzyme activity and GUS staining was performed on leaves with a diameter of one centimeter, and the observed color variations indicate differential effects of different *UTR*s on GUS translation. Different letters above the bars indicate significantly different values ($p < 0.05$) calculated by one-way analysis of variance (ANOVA) followed by Tukey's multiple range. **b** The fluorescence intensity indicates differential effects of different *UTR*s on eGFP translation. Scale bars = 100 μm. **c** Subcellular localization of two *BnABF4L*-CDS. Scale bars = 25 μm **d** Assessment of the transcriptional activation activity was carried out on two *BnABF4L*-CDS proteins. The pGBKT7 vector and *GAL4* gene were utilized as negative and positive controls, respectively. The measurement of β-galactosidase activities was conducted through X-α-gal staining

In the absence of ABA in the MS medium, growth of OE::*BnABF4L*-V1 is comparable to *Col* plants, with no significant difference in average root length. The average root length of OE::*BnABF4L*-V2 lines is approximately 56% of *Col*, while the average root length of OE::*BnABF4L*-V3 falls between OE::*BnABF4L*-V1 and OE::*BnABF4L*-V2. However, in the presence of 150 mM ABA MS medium, inhibition of germination in OE::*BnABF4L*-V1 and *Col* is not significant. In contrast, germination of OE::*BnABF4L*-V3 and OE::*BnABF4L*-V2 is significantly inhibited, resulting in shorter root lengths and smaller seedling sizes (Fig. 6a,b).

After eight hours of heat stress treatment, both *Col* and OE::*BnABF4L*-V1 exhibited severe wilting and leaf and stem shrinkage, indicating that the plants were on the verge of death. In contrast, the degree of leaf wrinkling in OE::*BnABF4L*-V2 and OE::*BnABF4L*-V3 was much less pronounced compared to col and OE::*BnABF4L*-V1. Furthermore, the stems of OE::*BnABF4L*-V2 and OE::*BnABF4L*-V3 remained upright, indicating that these two transgenic plants have a better ability to withstand high temperatures compared to *Col* and OE::*BnABF4L*-V1 (Fig. 6c).

Discussion

Oilseed rape (*Brassica napus* L.) is one of a crucial oil crop all over the world, facing various abiotic stresses throughout its growth cycle. Continued research into the stress resistance mechanisms of oilseed rape will aid in elucidating the molecular mechanisms by which

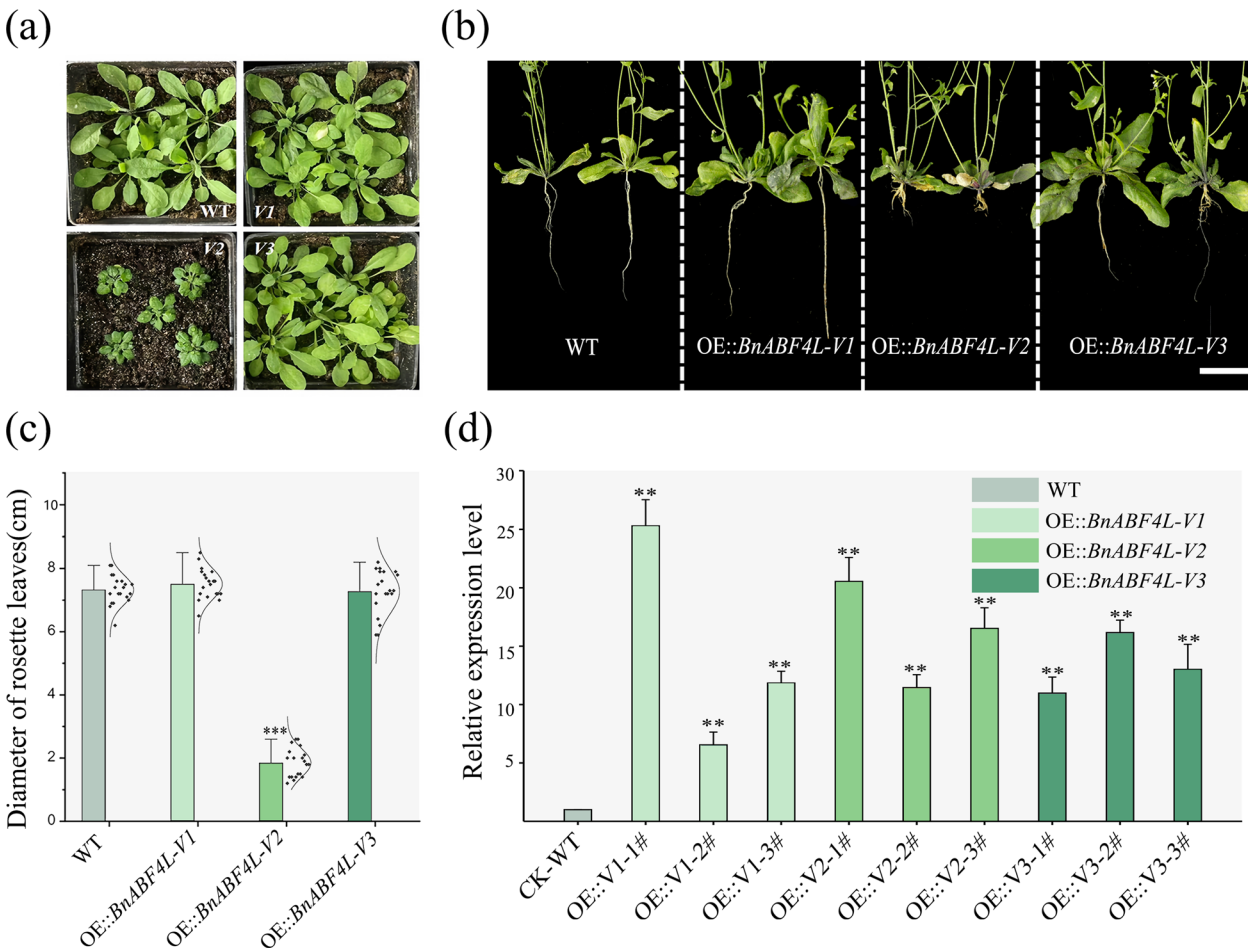

Fig. 5 Phenotypic comparison of *col* and three transgenic *Arabidopsis* in natural growth condition. **a** Comparison of phenotypes between four-week-old *Col* and transgenic plants overexpressing three transcripts of *BnABF4L*. Scale bars = 1 cm. **b** Root length of *Col* and different overexpression lines, scale bars = 2 cm. **c** Statistical analysis of rosette leaves diameter was performed, with error bars representing the standard error of the mean. **d** Relative expression level of *col* and different overexpression lines. (All the significance analysis were conducted by independent-samples *t*-test and black asterisks denote significance. ** $p < 0.01$, *** $p < 0.001$.)

plants adapt to adverse environments. A mutant of *B. napus*, *ndf2*, was derived from a high doubled haploid (DH) line *3529*. The seeds of this line were treated with diethyl sulfate and subjected to fast neutron bombardment[30]. Compared to its parental line *3529*, the *ndf2* exhibited enhanced resistance to abiotic stress (Fig. 1a).

ABA, a critical plant hormone, plays a key role in stress resistance[31]. ABA regulates physiological responses under adverse conditions, such as stomatal closure[32], root growth[33], and osmoregulation[34]. It also affects gene expression and metabolic activities through a complex signal transduction network, thereby enhancing the plant's stress tolerance[35]. Especially in the face of drought and salt stress, the activation of ABA signaling pathways is a crucial mechanism for plants to rapidly respond to and adapt to environmental changes.

ABF4 is an important transcription factor in the ABA signaling pathway and a member of the *ABF/AREB* gene family. Members of this gene family participate in the plant's response to various environmental stresses through key steps in the ABA signaling pathway[36]. Functional redundancy and complementarity among gene family members enable plants to flexibly respond to different adverse conditions, thus improving survival rates. For instance, *AtABF4* can bind to the promoter of *AtFYVE1* to activate its transcription, thereby regulating salt stress tolerance in *Arabidopsis* through a negative feedback loop[37]. *AtABF4* also regulates the transcription of *AtSOC1*, promoting flowering and inducing a drought escape response in *Arabidopsis*[38]. Additionally, *ABF4* can upregulate *SOX* expression to enhance tolerance to sulfites[39]. Hence, *ABF4* holds a central position in the ABA signaling pathway and interacts with other signaling

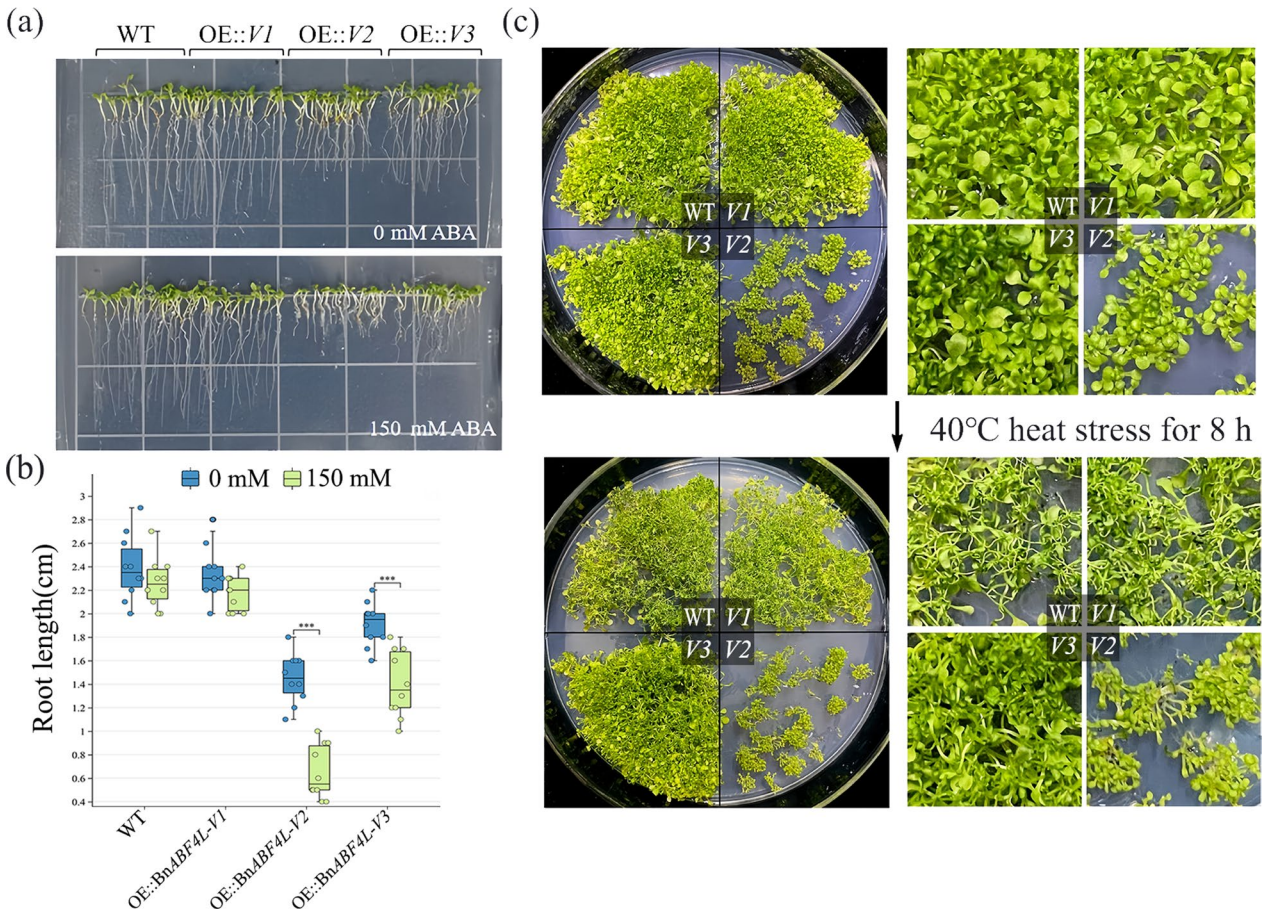

Fig. 6 Treatments of overexpressing *Arabidopsis* with ABA and heat stress. **a-b** Statistical analysis of root length in *Col* and three transgenic plants grown on MS medium containing 0 mM and 150 mM ABA for 10 days. (All the significance analysis were conducted by independent-samples *t*-test and black asterisks denote significance. ***$p < 0.001$.) **c** Comparison of the growth state of *Col* and three transgenic plants under heat stress for 8 h

pathways to form a complex network, further enhancing the plant's comprehensive response to adversity.

In this study, we identified 17 members of the *ABF4* gene family in *B. napus* (Fig. 1b) and analyzed their expression patterns in the transcriptome data of *3529* and *ndf2* (Fig. 1c). Using bioinformatics techniques, we found that most of these *ABF4* genes have conserved motifs and domains (Fig. 1e) and are extensively involved in the plant's response to both biotic and abiotic stresses and in hormone signaling pathways, thereby regulating plant growth and development (Fig. 1g). Through differential gene expression analysis, we identified *BnABF4L*, a gene whose expression level in *ndf2* was significantly higher than in *3529* (Fig. 1f**,** Fig. 2c). We thus infer that *BnABF4L* may play an important role in stress resistance and ABA signaling pathways in *B. napus*.

Research indicated that plants resist stress not only by regulating transcription factors and gene expression through the ABA signal transduction pathway but also by producing specific protein isoforms through alternative splicing (AS) at the post-transcriptional level[14]. This adaptability enhances their resilience to various environmental conditions. For example, abiotic stress signals can induce alternative splicing of *AtCIPK3*, producing different variants that interact with downstream genes and modulate ABA signaling through phosphorylation and negative regulation, thereby adjusting stress responses[40]. The *AtRPS4* gene adjusts its splicing pattern to varying levels of pathogen attack, conferring resistance[41]. In rice, the *OsDR11* gene undergoes alternative splicing to generate long and short mRNA isoforms, with the long isoform enhancing resistance to blast fungus, while the short isoform counteracts this function[42]. Additionally, *AtSAD1* encodes a homolog of *LSm5*, and under drought and ABA stress, the sad1/lsm5 mutant exhibits reduced U6 snRNP abundance, leading to the accumulation of pre-mRNAs[43]. Through cloning and sequencing, we identified that the *BnABF4L* in normal growth conditions can produce three transcripts via alternative splicing,

which we named *BnABF4L*-V1, *BnABF4L*-V2, and *BnABF4L*-V3 (Fig. 2b). Interestingly, studies indicated that the proportion of stress-induced alternative splicing types, such as A3SS, is extremely low in *Arabidopsis*, constituting less than 5% of all AS events[44]. However, all three splicing events of *BnABF4L* are of the A3SS type. Currently, the factors influencing splice site selection are not well understood, necessitating further evidence to elucidate the relationship between stress conditions, sequences, and splice sites.

In this study, we analyzed the relative expression levels of *ABF4L* transcripts in *B. napus* grown under normal and stress conditions. We found that in the more stress-resistant *ndf2* mutant, V2 consistently dominated, with its expression level higher than that of the other two transcripts (Fig. 2c). Interestingly, as the duration of stress increased, the expression level of V1 gradually decreased, while V3's expression proportion increased (Fig. 3). This suggested that under stress conditions, *BnABF4L* adjusts the ratio of different transcripts through alternative splicing, shifting more pre-mRNA towards forming the V3 transcript in response to stress.

Sequence alignment revealed that the CDS encoded by V1 and V2 are completely identical, whereas the CDS encoded by V3 is shorter (Fig. 2a). We thus designated these two CDS sequences as *BnABF4L*-CDS*l* (CDS-*long*) and *BnABF4L*-CDS*s* (CDS-*short*) respectively. Subcellular localization and yeast transcription activation assays indicated that both proteins were localized in the cell nucleus and possessed transcriptional activity (Fig. 4c,d). Based on above results, we preliminarily identified them as a class of bZIP-type transcription factors.

We found that the 5'UTR of V1 contains seven AUG codons (Fig. 2b), which may give rise to upstream open reading frames (uORFs)[45]. uORFs are translation regulatory elements present in the non-coding region of eukaryotic mRNAs and have an inhibitory effect on the translation of the main coding region, known as the primary open reading frame (pORF)[46]. We fused the three different 5'UTRs to the 35S promoter to drive the expression of a reporter gene. By detecting the reporter gene's expression, we investigated the influence of different 5'UTRs on translation. The results indicated that under similar transcript levels for the three variants, the 5'UTR of V1 strongly inhibits translation to the extent that V1 almost loses its biological function, while the translation of V2 and V3 is not significantly affected (Fig. 4a,b). Under stress conditions, the pre-mRNA intended to be spliced into V1 is more often spliced into V3 (Fig. 3). We speculate that this process is likely regulated by environmental stress, which affects the expression of uORFs located in the 5'UTR of V1, thereby strongly inhibiting V1-pORF translation and resulting in increased relative abundance of V3.

Research has shown that overexpression of *AtABF4* in *Arabidopsis* enhances the plant's sensitivity to ABA, thereby inhibiting root cell elongation and resulting in a dwarf phenotype. We expressed the three transcripts of *BnABF4L* in *Arabidopsis*. The results demonstrated that the growth and development of the aerial parts in OE::*BnABF4L*-V1 and OE::*BnABF4L*-V3 were almost unaffected, while the growth and development of OE::*BnABF4L*-V2 transgenic plants were significantly inhibited, resulting in dwarf plants with short, round leaves (Fig. 5a,c). The root phenotypes of different transgenic overexpression lines also varied. OE::*BnABF4L*-V2 and OE::*BnABF4L*-V3 had notably shorter roots, with OE::*BnABF4L*-V2 showing more pronounced inhibition than OE::*BnABF4L*-V3 (Fig. 5b). When subjected to ABA and heat stress, the results showed that on medium containing 150 mM ABA, the root length of *Col-0* and OE::*BnABF4L*-V1 plants was slightly shorter, but not significantly so (Fig. 6a,b). In contrast, overexpression of V2 and V3 increased plant sensitivity to ABA, with their root lengths significantly inhibited, and OE::*BnABF4L*-V2 showing the highest sensitivity. Heat stress results also indicated that OE::*BnABF4L*-V2 and OE::*BnABF4L*-V3 were more heat-tolerant (Fig. 6c). Moderate increases in endogenous ABA levels can enhance plant salt and drought tolerance; however, high concentrations of ABA can also inhibit root elongation[33].

Based on the above experimental results, we established the following model: the alternative splicing of the *BnABF4L* may provide a flexible regulatory mechanism for the ABA signaling pathway. B*nABF4L* generates functionally differentiated transcripts through alternative splicing, combined with translation control mediated by 5'UTR. This post-transcriptional modulation dynamically adjusting protein expression patterns at post transcription and translation levels, thereby prioritizing the expression of highly efficient stress resistant variants (V2/V3) under stress conditions while avoiding excessive growth inhibition. This mechanism provides efficient and reversible regulatory strategies for plants to cope with complex environments. Under normal growth conditions, the *BnABF4L* produces three different transcripts through alternative splicing: *BnABF4L*-V1, *BnABF4L*-V2, and *BnABF4L*-V3, with V2 having the highest relative expression level, followed by V1 and V3. Both V1 and V2 encode CDS*l*, while V3 encodes a shorter protein variant, CDS*s*. This variation in protein length likely implies functional diversification, with each transcript variant playing a unique role in the plant's physiological processes. In environments

with abiotic stress, uORF in the 5'UTR of V1 might be induced, strongly inhibiting the translation of pORF of V1. This inhibition significantly reduces the production of the V1 protein, subsequently generating V2 and V3 transcripts. As a result, the overall level of CDS*l* slightly increases, while the level of CDS*s* significantly increases. This splicing switch enhances the production of V2 and V3, which can participate in the ABA signaling pathway, and their overexpression increases the plant's sensitivity to ABA, thereby enhancing the plant's stress resistance (Fig. 7a).

However, it is noteworthy that overexpression of V2 can lead to significant changes in plant morphology and root structure, causing severe variation. In contrast,

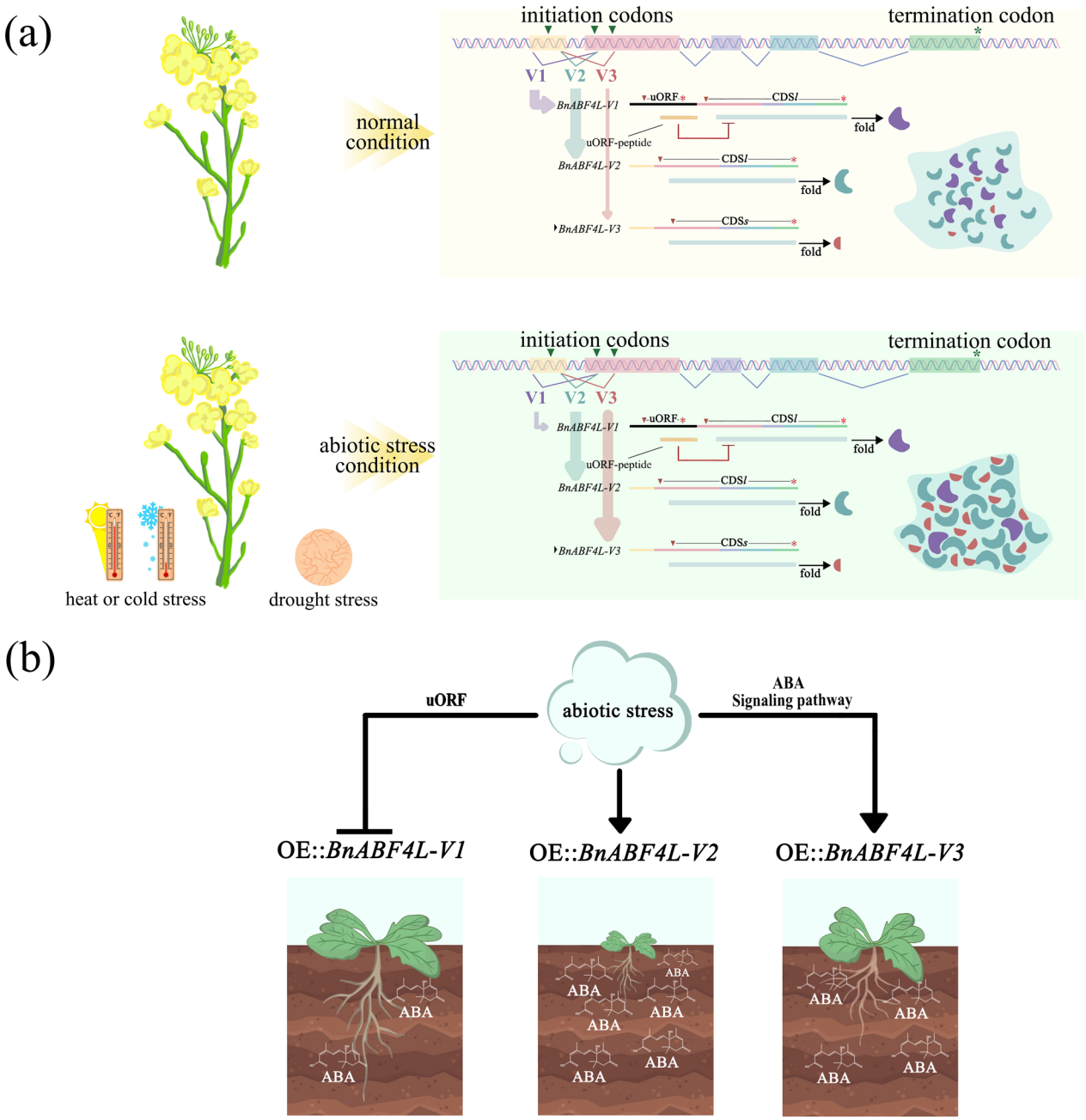

Fig. 7 Model of flexible regulatory mechanism of alternative splicing events of *BnABF4L* under environmental stress. **a** AS events of *BnABF4L* in *B. napus* under different growth conditions. **b** Mechanisms of the impact of different AS variants on plant growth and development and response to abiotic stress

V3, while slightly altering root length, has minimal impact on overall plant growth and development. This ensures that under stress conditions, the plant's growth is not excessively inhibited by the elevated expression of V2, while the increased expression of V3 can assist V2, enhancing the plant's stress resistance without significantly inhibiting growth (Fig. 7b).

This regulatory mechanism highlights the importance of AS and untranslated region elements in plant stress responses. By adjusting the expression levels of different transcripts, the *BnABF4L* adapts to environmental changes, optimizing the plant's ability to withstand abiotic stress and participating in the regulation of growth and development. This not only indicates that alternative splicing may play a crucial role of alternative splicing in plant responses to abiotic stress but also expands the regulatory mechanisms of the ABA signaling pathway, providing theoretical foundations and technical support for breeding stress-resistant varieties.

Conclusion

The present study comprehensively investigated the regulatory function of alternative splicing (AS) within the abscisic acid (ABA) signaling pathway in Brassica napus, with the objective of advancing the development of stress-resistant breeding strategies. Through the identification of 17 *ABF4* homologs and the analysis of their conserved motifs, domains, and promoter cis-elements, we elucidated their potential roles in hormone signaling and stress adaptation. Transcriptome profiling identified *BnABF4L* as a significantly differentially expressed gene in the stress-tolerant mutant *ndf2*, exhibiting distinct expression dynamics compared to its parental line *3529*.

Further investigation revealed that *BnABF4L* undergoes alternative splicing (AS) of the A3SS type under abiotic stress, generating three transcript variants (V1, V2, V3) with divergent 5'UTRs and coding sequences. Functional assays demonstrated that the 5'UTR of V1, which contains upstream open reading frames (uORFs), strongly inhibits translation, while V2 and V3 promote efficient protein synthesis. Overexpression studies in Arabidopsis showed that V2 enhances ABA sensitivity and heat tolerance but compromises growth, whereas V3 balances stress resilience with minimal impact on development.

Our findings establish a model in which *BnABF4L* fine-tunes stress responses through AS-mediated shifts in transcript ratios. Under stress conditions, preferential splicing toward V3 and suppression of V1 mitigate translational inhibition, enabling adaptive expression of functional isoforms. This mechanism underscores the dual role of AS and uORFs in optimizing stress adaptation while preserving growth plasticity. This work not only elucidates a novel regulatory layer in ABA signaling but also provides actionable targets for engineering stress-resilient rapeseed varieties. Future research should focus on exploring the upstream splicing regulators of *BnABF4L* and validating its agronomic potential under field conditions, thereby paving the way for precision breeding in crops facing climate challenges.

Materials and methods

Plant materials and growth conditions

Seed of *B. napus* strains *3529* and *ndf2* were obtained from Wei[30], *Col-0 Arabidopsis* and *N. benthamiana* were preserved in our lab. Except for the abiotic stress treatments, all plants were grown in a controlled environment chamber with a constant temperature of 25 °C, subjected to a light cycle of 16 h on and 8 h off.

Identification and classification of *ABF4* gene family members in *B. napus* and the other plants

To obtain all the *ABF4* gene family members, bidirectional blast alignment and Hidden Markov Model (HMM) search were conducted. NCBI's BLAST algorithm was used for alignments and homology analyses (e-value =1e-10). Additionally, *ABF4* gene family members were identified using hmmer3 software (e-value =1e-5), based on the HMM of the conserved domains bZIP_1 (PF00170) from the Pfam Database. The results of the blast alignment and the HMM search were then merged, and duplicate values were removed. All the data information was listed in Supplementary Table S1.

Phylogenetic tree construction

To investigate the evolutionary relationships among *ABF4* gene family members in *B. napus*, a total of 17 full-length ABF4 protein sequences were extracted. These sequences included representatives from ABF1, ABF2, ABF3, and ABF4 proteins in *Arabidopsis*, as well as ABF4 proteins from *N. benthamiana*, *S. lycopersicum*, *V. vinifera*, and *Z. mays* (Table S1). The Multiple sequence alignments were then subjected to the maximum likelihood (ML) method for constructing the phylogenetic tree using MEGA-X software. Finally, the phylogenetic tree was visualized using Chiplot (https://www.chiplot.online/).

Gene structures, motifs, conserved domains and promoter region *cis*-elements analyses

The conserved motif structures were analyzed using the MEME online tool (Supplementary Figure S2). The conserved domain was obtained, and motif function was analyzed through the NCBI-CDD database. To analyze the promoters, a 1500 bp sequence upstream of the ATG start codon of *ABF4* genes was extracted.

The *cis*-elements of the promoters were analyzed using PlantCare (Supplementary Table S2). Visualization of all the data was performed using TBtools[47].

Vector construction

In this study, a total of five vector backbones were utilized. These included vectors for subcellular localization analysis of CDS*l* and CDS*s* (pBI221-eGFP), as well as vectors for assessing their transcriptional activation function (pGBKT7). The effects of the different 5'UTRs of the three transcripts on reporter gene translation (pBI121-eGFP and pBI121-GUS). Additionally, the phenotypic characteristics of overexpressing all three transcript variants in *Arabidopsis* were determined using the pFGC-5941 vector.

All the recombinant plasmids were constructed by seamless DNA cloning.

All primers used were provided in Supplementary Table S4.

RNA extraction and qRT-PCR

To analyze *ABF4 s* expression in various *B. napus* tissues, RNA-Seq datasets from strain *3529* and *ndf2* were utilized. Each tissue sample had two biological replicates, with two technical replicates for each sequencing sample (Supplementary Table S3).

Total RNA from *B. napus* and *Arabidopsis* was extracted employing FastPure Universal Plant Total RNA Isolation Kit (Vazyme, RC411-01) according to guidelines.

Quantitative real-time PCR (qRT-PCR) analysis was conducted to validate RNA-seq data. *BnABF4L* and its variants (V1, V2, and V3) were analyzed using the qPCR SYBR Green Master Mix Kit (YEASEN Biotech) across two biological and three technical repeats. To distinguish between different splice variants, the primers were designed with specific locations, as detailed in the Supplementary Figure S3.

The qRT-PCR cycle parameters were set as 95 °C for 30 s, followed by 40 cycles of 5 s at 95 °C and 15 s at 58 °C, with a final melting curve spanning from 65 to 95 °C in 0.5 °C increments, and relative gene expression levels were determined using the $2^{-\Delta\Delta Ct}$ method with β-actin from *B. napus*.

Comparison between RNA-seq and qRT-PCR data was performed using Student's *t*-test and Pearson correlation coefficient.

Subcellular localizations of *BnABF4L-CDSl* and *BnABF4L-CDSs*

To investigate the impact of different splicing modes or sites on gene localization and the potential of *ABF4L* as a transcription factor, *ABF4L*-CDS*l* and *ABF4L*-CDS*s* were inserted into the pBI221 vector upstream of the *eGFP* reporter gene, driven by the CaMV35S promoter. *N. benthamiana* leaves were enzymatically treated, and protoplasts were collected and mixed with recombinant plasmid and PEG solution. After incubation, transformation was stopped, and the protoplasts were examined using a confocal laser microscope. All solution compositions are provided in Supplementary Table S5.

Transactivation assay in yeast cells

The yeast strain AH109, harboring the HIS3 and lacZ reporter genes with three and four GAL4 binding elements in their promoters, respectively, served as the assay system. *ABF4L*-CDS*l* and *ABF4L*-CDS*s* were cloned into the pGBKT7 vector containing the GAL4 DNA-binding domain to generate plasmids for transcriptional activation testing.

Two recombination plasmids, the positive control pGAL4, and the negative control pGBKT7, were transformed into AH109. Transformants were plated on YPDA and SD/-Trp-His plates, and their growth status was assessed to evaluate transcriptional activation activities. Transfected yeast cells were also transferred onto filter paper and incubated at 30 °C for 3–5 h in the presence of X-α-gal to assess β-galactosidase activity by observing the development of a blue color.

Qualitative and quantitative analysis of the effect of three 5'UTRs on reporter genes' translation efficiency

To assess the translation efficiency of reporter genes, recombinant plasmids pBI121-5'UTRs-eGFP and pBI121-5'UTRs-GUS were separately transformed into *Agrobacterium tumefaciens*. Positive monoclonal colonies were selected and cultured until reaching an OD600 = 1.2. They were then resuspended in suspension buffer to reach an OD600 = 0.8 and injected into tobacco leaves. After three days of cultivation, fluorescence intensity and GUS staining intensity were observed for each sample.

To quantify the effects of the transcript variants on protein expression, we ensured consistent expression levels of the fusion gene fragments at the transcriptional level using qPCR. We selected tobacco leaves with similar GUS expression levels determined by GUS enzyme activity in the transiently transformed material (Supplementary Figure S4).

Initially, total protein concentration was measured, and a series of bovine serum albumin (BSA) gradient solutions were prepared and their absorbance values recorded to generate a standard curve. Subsequently, fluorescence values of 4-methylumbelliferyl-β-D-glucuronide (4-MUG) standard gradient solutions were measured at 0.5 h of reaction to generate another

standard curve for 4-methylumbelliferone (4-MU) concentrations.

The absorbance values of the protein samples were then used with the BSA concentration standard curve to determine protein concentration. The GUS enzyme catalyzes the hydrolysis of 4-MU, which fluoresces at 455 nm. By using the standard curve of 4-MU concentrations, we measured the concentration of 4-MU in the reaction system after 0.5 h of reaction.

ABA and abiotic stress treatments

To examine the impact of abiotic stresses on the translation efficiency of *ABF4L* and its transcript variants in the stress-tolerant strain *ndf2*, plants were subjected to different stress treatments. For extreme temperature stress, plants were exposed to either 2 °C or 40 °C with a 16-h light and 8-h dark photoperiod. Samples were collected at 0, 3, 6, 9, and 12 h. For drought and osmotic stress, nutrient solutions were replaced with solutions containing 200 mM mannitol and 20% PEG-6000. Samples were collected at 0, 3, 6, 9, 12, 24, and 48 h.

To investigate the effects of transcript variants on plant growth and stress response, stable transformation was achieved by infiltrating constructs into *Arabidopsis* using the floral dip method. Bacterial cultures harboring recombinant plasmids were prepared and introduced into *Col-0 Arabidopsis*. Transgenic plants were screened and subjected to treatments with 150 mM ABA and high temperature stress at ten days old.

Statistical analyses

All treatments described in this study comprised a minimum of three independent biological and technical replicates. All statistical analyses were performed using OriginPro version 2021 for Windows.

Abbreviations

ABA	Abscisic acid
ABF4	ABRE BINDING FACTOR 4
ABRE	ABA responsive element
AS	Alternative splicing
CDSl	BnABF4L-CDS-long
CDSs	BnABF4L-CDS-short
uORF	Upstream open reading frames
pORF	Protein-coding open reading frame
3′UTR	3′ Untranslated region
5′UTR	5′ Untranslated region

Supplementary Information

The online version contains supplementary material available at https://doi.org/10.1186/s13068-025-02645-2.

Additional file 1
Additional file 2
Additional file 3
Additional file 4
Additional file 5
Additional file 6

Acknowledgements

We would like to acknowledge all researchers in our laboratory for their help.

Author contributions

M.Wang, R.Z. and C.Y. designed the experiments and wrote the paper; R.W. conducted the experiments; S.W., X.L, M.Wu. and Z.X. did the experiments and analyzed the data; M.Wang revised and improved the manuscript. All authors reviewed the manuscript.

Funding

Sichuan Science and Technology Program (2021YFYZ0027), The National Key Research and Development Program of China (2023YFD1200202), the Provincial Science and Technology Department project (SCCXTD-2024–3, 2022ZDZX0015 and 2021YFYZ0018-LH) and the Deyang municipal Key Research and Development Project (2021 NZ043).

Availability of data and materials

No datasets were generated or analysed during the current study.

Declarations

Ethics approval and consent to participate

Our research did not involve any human or animal subjects, materials, or data. We owned the plant materials and we have permissions to use them. We declare that the collection and use of plant materials in this study complies with relevant institutional, national, and international guidelines and legislation.

Consent for publication

Not Applicable.

Competing interests

The authors declare no competing interests.

Received: 18 November 2024 Accepted: 31 March 2025
Published online: 08 May 2025

References

1. Gu J, T, et al. The story of a decade: Genomics, functional genomics, and molecular breeding in *Brassica napus*. Plant Communications. 2024. https://doi.org/10.1016/j.xplc.2024.100884.
2. Lohani N, et al. Engineering Multiple Abiotic Stress Tolerance in Canola, *Brassica napus*. Front Plant Sci. 2020. https://doi.org/10.3389/fpls.2020.00003.
3. Lee S, et al. Overlapping activities of ELAV/Hu RNA binding proteins specify multiple neural alternative splicing programs. Cold Spring Harbor Laboratory. 2020;80(1):140–55. https://doi.org/10.1016/j.molcel.2020.09.007.
4. Ner-Gaon H, et al. Intron retention is a major phenomenon in alternative splicing in *Arabidopsis*. Plant J. 2004;39(6):877–85. https://doi.org/10.1111/j.1365-313X.2004.02172.x.
5. Wright CJ, Smith CWJ, Jiggins CD. Alternative splicing as a source of phenotypic diversity. Nat Rev Gene. 2022;23(11):697–710. https://doi.org/10.1038/s41576-022-00514-4.
6. Wang X, et al. An exon skipping in a *SEPALLATA-Like* gene is associated with perturbed floral and fruits development in cucumber. J Integr Plant Biol. 2016;58(9):766–71. https://doi.org/10.1111/jipb.12472.
7. Cui Y, et al. Prediction and feature analysis of intron retention events in plant genome. Comput Biol Chem. 2017;68:219–23. https://doi.org/10.1016/j.compbiolchem.2017.04.004.

8. Zhenxun, et al. Exon-centric regulation of pyruvate kinase M alternative splicing via mutually exclusive exons. J Molr Cell Biol. 2011;4(2):79–87. https://doi.org/10.1093/jmcb/mjr030.
9. Gallinaro H, Domenjoud L, Jacob M. Structural study of the 5′ end of a synthetic premessenger RNA from adenovirus. Evidence for a long-range exon-intron interaction. J Mol Biol. 1994;240(3):205–25. https://doi.org/10.1006/jmbi.1994.1436.
10. Lou H, Mccullough AJ, Schuler MA. 3′ splice site selection in dicot plant nuclei is position dependent. Mol Cell Biol. 1993;13(8):4485–93. https://doi.org/10.1128/mcb.13.8.4485-4493.1993.
11. Kitagawa N, et al. Computational analysis suggests that alternative first exons are involved in tissue-specific transcription in rice (*Oryza sativa*). Bioinformatics. 2005;21(9):1758–63. https://doi.org/10.1093/bioinformatics/bti253.
12. Tien JF, et al. *CDK12* regulates alternative last exon mRNA splicing and promotes breast cancer cell invasion. Nucleic Acids Res. 2017;45(11):6698–716. https://doi.org/10.1093/nar/gkx187.
13. Marasco LE, Kornblihtt AR. The physiology of alternative splicing. Nat Rev Mol Cell Biol. 2022;24(4):242–54. https://doi.org/10.1038/s41580-022-00545-z.
14. Punzo P, Grillo S, Batelli G. Alternative splicing in plant abiotic stress responses. Biochem Soc Trans. 2020;48(5):2117–26. https://doi.org/10.1042/BST20200281.
15. Capovilla, et al. *PORCUPINE* regulates development in response to temperature through alternative splicing. Nature Plants. 2018;4(8):534–9. https://doi.org/10.1038/s41477-018-0176-z.
16. Cheng Q, et al. An alternatively spliced heat shock transcription factor, *OsHSFA2dI*, functions in the heat stress-induced unfolded protein response in rice. Plant Biol. 2015;17(2):419–29. https://doi.org/10.1111/plb.12267.
17. Ule J, Blencowe BJ. Alternative splicing regulatory networks: functions, mechanisms, and evolution. Mol Cell. 2019;76(2):329–45. https://doi.org/10.1016/j.molcel.2019.09.017.
18. Rai GK, et al. Unlocking nature's stress buster: Abscisic acid's crucial role in defending plants against abiotic stress. Plant Stress. 2024. https://doi.org/10.1016/j.stress.2024.100359.
19. Pan X, et al. Identification of ABF/AREB gene family in tomato (*Solanum lycopersicum* L) and functional analysis of ABF/AREB in response to ABA and abiotic stresses. PeerJ. 2023. https://doi.org/10.7717/peerj.15310.
20. Choi HI, et al. ABFs, a family of aba-responsive element binding factors. J Biol Chem. 2000;275(3):1723–30. https://doi.org/10.1074/jbc.275.3.1723.
21. Li F, et al. Genome-wide analysis of the *AREB/ABF* gene lineage in land plants and functional analysis of *TaABF3* in *Arabidopsis*. BMC Plant Biol. 2020;20(1):558. https://doi.org/10.1186/s12870-020-02783-9.
22. Yoshida T, et al. Four *Arabidopsis AREB/ABF* transcription factors function predominantly in gene expression downstream of *SnRK2* kinases in abscisic acid signaling in response to osmotic stress. Plant, Cell Environ. 2014;38(1):35–49. https://doi.org/10.1111/pce.12351.
23. Yoshida T, et al. Functional analysis of a bZIP-type transcription factor, ABF1, involved in ABA signaling in response to water stress. Plant and Cell Physiology Supplement. 2011. https://doi.org/10.14841/jspp.2011.0.0945.0.
24. Guan Y, et al. Low temperature stress-induced perception and molecular signaling pathways in plants. Environ Exp Botany. 2023. https://doi.org/10.1016/j.envexpbot.2022.105190.
25. Orellana S, et al. The transcription factor *SlAREB1* confers drought, salt stress tolerance and regulates biotic and abiotic stress-related genes in tomato. Plant, Cell Environ. 2010;33(12):2191–208. https://doi.org/10.1111/j.1365-3040.2010.02220.x.
26. Fujita Y, et al. ABA-mediated transcriptional regulation in response to osmotic stress in plants. J Plant Res. 2011;124(4):509–25. https://doi.org/10.1007/s10265-011-0412-3.
27. Li L, et al. *PDC1* is activated by *ABF4* and inhibits seed germination by promoting ROS accumulation in *Arabidopsis*. Environ Exp Bot. 2022;206:105188. https://doi.org/10.1016/j.envexpbot.2022.105188.
28. Natalia R, et al. The functional meaning of 5′UTR in protein-coding genes. Int J Mol Sci. 2023;24(3):2976. https://doi.org/10.3390/ijms24032976.
29. Preussner M, et al. Splicing-accessible coding 3′UTRs control protein stability and interaction networks. Genome Biol. 2020;21(1):186. https://doi.org/10.1186/s13059-020-02102-3.
30. Maolin W, et al. A gain-of-function mutant of *IAA7* inhibits stem elongation by transcriptional repression of *EXPA5* genes in *Brassica napus*. Int J Mol Sci. 2021;22(16):9018. https://doi.org/10.3390/ijms22169018.
31. Waadt R, et al. Plant hormone regulation of abiotic stress responses. Nat Rev Mol Cell Biol. 2022;23(7):680–94. https://doi.org/10.1038/s41580-022-00479-6.
32. Bharath P, Gahir S, A.S.J.F.i.P.S. Raghavendra. Abscisic acid-induced stomatal closure: an important component of plant defense against abiotic and biotic stress. Front Plant Sci. 2021;4(12):615114. https://doi.org/10.3389/fpls.2021.615114.
33. Teng Z, et al. Effects of stress-induced ABA on root architecture development: positive and negative actions. The Crop Journal. 2023;11(4):1072–9. https://doi.org/10.1016/j.cj.2023.06.007.
34. Huijuan G, et al. Up-regulation of abscisic acid signaling pathway facilitates aphid xylem absorption and osmoregulation under drought stress. J Exp Bot. 2016;67(3):681–93. https://doi.org/10.1093/jxb/erv481.
35. Muhammad Aslam M, et al. Mechanisms of abscisic acid-mediated drought stress responses in plants. Int J Mol Sci. 2022;23(3):1084. https://doi.org/10.3390/ijms23031084.
36. Kim SY. The role of *ABF* family bZIP class transcription factors in stress response. Physiol Plant. 2005;126(4):519–27. https://doi.org/10.1111/j.1399-3054.2005.00601.x.
37. Pan W, et al. The effect of ABRE BINDING FACTOR 4-mediated FYVE1 on salt stress tolerance in *Arabidopsis*. Plant Sci. 2020;296: 110489. https://doi.org/10.1016/j.plantsci.2020.110489.
38. Hwang K, et al. *Arabidopsis ABF3* and *ABF4* transcription factors act with the NF-YC complex to regulate *SOC1* expression and mediate drought-accelerated flowering. Mol Plant. 2019;12(4):489–505. https://doi.org/10.1016/j.molp.2019.01.002.
39. Yu Z-D, et al. ABA promotes sulfite stress tolerance by ABF4-mediated upregulation of SOX expression. Environ Exp Bot. 2022;203: 105070. https://doi.org/10.1016/j.envexpbot.2022.105070.
40. Sanyal SK, et al. Alternative splicing of *CIPK3* results in distinct target selection to propagate ABA signaling in *Arabidopsis*. Front Plant Sci. 2017;8:1924. https://doi.org/10.3389/fpls.2017.01924.
41. Zhang XC, Gassmann W. Alternative splicing and mRNA levels of the disease resistance gene *RPS4* are induced during defense responses. Plant Physiol. 2007;145(4):1577–87. https://doi.org/10.1104/pp.107.108720.
42. Duan L, et al. Two different transcripts of a *LAMMER* kinase gene play opposite roles in disease resistance. Plant Physiol. 2016;172(3):1959–72. https://doi.org/10.1104/pp.16.01245.
43. Cui P, et al. Dynamic regulation of genome-wide pre-mRNA splicing and stress tolerance by the Sm-like protein LSm5 in *Arabidopsis*. Genome Biol. 2014;15(1):R1. https://doi.org/10.1186/gb-2014-15-1-r1.
44. Zhu FY, et al. Proteogenomic analysis reveals alternative splicing and translation as part of the abscisic acid response in *Arabidopsis* seedlings. Plant J. 2017;91(3):518–33. https://doi.org/10.1111/tpj.13571.
45. Wang J, Liu J, Z.J.T.i.P.S. Guo. Natural uORF variation in plants. Trends in Plant Sci. 2024;29(3):290–302. https://doi.org/10.1016/j.tplants.2023.07.005.
46. Dever TE, Ivanov IP, Hinnebusch AG. Translational regulation by uORFs and start codon selection stringency. Genes Dev. 2023;37(11–12):474–89. https://doi.org/10.1101/gad.350752.123.
47. Chen C, et al. TBtools-II: A "one for all, all for one" bioinformatics platform for biological big-data mining. Mol Plant. 2023;16(11):1733–42. https://doi.org/10.1016/j.molp.2023.09.010.

Publisher's Note